

# Experimental FTIR and Theoretical Investigation of the Molecular Structure and Vibrational Spectra of Terephthaloyl Chloride by Density Functional Theory

Yunusa Umar<sup>a</sup> and Sahar Abdalla<sup>b</sup>

<sup>a</sup>Department of Chemical and Process Engineering Technology, Jubail Industrial College  
POBox 10099, Jubail Industrial City- 31961, Saudi Arabia.

<sup>b</sup>Department of Chemistry, University of Khartoum, Khartoum, Sudan

---

**Abstract:** The FTIR spectrum of terephthaloyl chloride was recorded and analyzed. The optimized molecular structures, harmonic vibrational wavenumbers, and corresponding vibrational assignments of the terephthaloyl chloride are theoretically examined by using the Becke-3-Lee-Yang-Parr (B3LYP) density functional theory (DFT) method together with the standard 6-311++G(d,p) basis set. The geometrical and thermodynamic parameters, highest occupied and lowest unoccupied molecular orbitals (HOMO and LUMO), Infrared intensities, Raman activities and molecular electrostatic potential results are reported. In addition, reliable vibrational assignments have been made on the basis of potential energy distribution (PED) using VEDA4 program. Simulated IR and Raman spectra are compared with the experimental FTIR and FT-Raman spectra.

**Keywords:** Terephthaloyl chloride, FTIR, PED, Vibrational Spectra, HOMO and LUMO.

---

## I. Introduction

Terephthaloyl chloride (TPC, benzene-1,4- dicarbonyl chloride) is the acid chloride of terephthalic acid and is used as a key component for the production of aromatic polyamides (aramids), where it imparts flame resistance, chemical resistance, temperature stability, light weight, and very high strength [1-5]. The aromatic polyamides are used in advanced technologies and have been transformed into flame resistance, chemical resistance, thermally stable and very high strength fibers and coatings that are widely utilized in the aerospace, bullet-proof body armor, sport fabrics, protective clothing, electric installations, industrial filters, etc. [2]. TPC is also an effective water scavenger, used to stabilize isocyanates and urethane prepolymers [1]. In addition, TPC is used as a co-monomer and cross-linking agent to produce different types of polymers [6-12].

Despite the wide applications of terephthaloyl chloride, to the best of our knowledge, there is no detailed theoretical study present in the literature about the structural, electronic and vibrational properties of terephthaloyl chloride. Such study will not only aid in making definitive assignment of the fundamental normal modes and in clarifying experimental data but will also be helpful in context of further studies of this molecule. The B3LYP density functional theory calculations exhibit good performance on the molecular geometry and vibrational properties of organic compounds [13-20]. Thus, the aim of this work is to take advantage of the quantum-mechanical calculations to carry out systematic study on the molecular structure and vibrational spectra which will give depth insight in understanding the properties of the title molecule and aid in clarifying and complementing available experimental data. This paper will reveal additional quantitative chemical knowledge and detailed insight about the molecular structure, thermodynamic properties, vibrational spectra and assignments of vibrational mode of terephthaloyl chloride.

## II. Experimental Details

A commercial sample of terephthaloyl chloride with about 99% purity was purchased from Sigma-Aldrich Chemical Company and was used without further purification. FT-IR spectrum was recorded in the region of 4000 – 400 cm<sup>-1</sup> using Shimadzu FTIR Prestigi-21 spectrophotometer with KBr pellets at a resolution of 4.0 cm<sup>-1</sup>. The experimental Raman spectrum of terephthaloyl chloride was obtained from the spectra database for organic compounds, SDBS website [21].

## III. Computational Details

Gaussian 03 program package [22] was used to optimize the structure, predict energy, and calculate thermodynamic parameters, atomic charges and vibrational wavenumbers of terephthaloyl chloride. Computations were performed using Density Functional Theory (DFT) adopting Becke's three-parameter exchange functional [23] combined with Lee-Yang-Parr [24] correlation functional (B3LYP) methods. The standard 6-311++G(d,p) basis set was used for all the atoms to carry out the calculations utilizing the C<sub>2v</sub> symmetry of the title compound. The vibrational IR and Raman data are reported, and each of the vibrational

modes was visually confirmed by Gauss-View program [25]. The VEDA4 program [26] was used to characterize the normal vibrational modes on the basis of Potential Energy Distribution (PED). The wavenumbers and intensities obtained from the computation were used to simulate infrared and Raman spectra. In addition, the highest occupied molecular orbital (HOMO) and lowest unoccupied molecular orbital (LUMO) energy values, HOMO-LUMO energy gap, molecular electrostatic potential (MEP) for TPC were calculated using the same level of theory.

## IV. Result and Discussion

### 4.1 Molecular Geometry

The molecular structure of TPC which consists of a phenyl ring along with two carbonyl chloride groups belongs to  $C_{2v}$  point group symmetry. The structure of TPC is optimized by Berny's optimization algorithm incorporated in Gaussian 03 program. The equilibrium structure along with the numbering of atoms of TPC calculated at B3LYP/6-311++G(d,p) level of theory is given in Fig. 1. The optimized geometrical parameters (bond lengths, bond and dihedral angles) of the title molecule are given in Table 1. The entire atoms of the TPC molecule belong to the same plane, even though it contains two carbonyl chloride groups. However, the hexagonal structure of the base molecule is slightly distorted due to the substitution of the carbonyl chloride groups into the ring.

All the C-C bond lengths in the phenyl ring of the TPC which are slightly stretched out fall in a range of 1.385 – 1.404 Å. The ring CCC angles are slightly smaller than 120° at the points of substitution and longer than 120° at other positions. The four C-H bonds in the ring have almost equal inter nuclear distance and have been calculated to be around 1.081 Å. The change in the phenyl ring C-H bond's length on substitution is attributed to change in charge distribution of the carbon atoms in phenyl ring [27, 28]. The carbon atoms in phenyl ring are sigma bonded to hydrogen atoms and substitution of carbonyl chloride groups for hydrogen atoms reduce the electron density at ring carbon atoms. Thus, in substituted benzenes, the ring carbon atoms exert a large attraction on the valence electron cloud of the H atoms resulting in the increase in the C-H force constant and a decrease in corresponding bond length. The two C=O of the TPC have the same bond lengths (1.187 Å) typical of double bond character. Similarly, the two C-Cl has the same bond length which is calculated to be 1.819 Å.

### 4.2 Vibrational Spectra

The optimized structural parameters were used to compute the vibrational wavenumbers for the title compound at B3LYP/6-311++G(d,p) level of theory. Since DFT hybrid B3LYP functional tends to overestimate the fundamental modes, the calculated vibrational wavenumbers are usually higher than the observed vibrational modes, and the differences are accounted for by using scaling factor. Therefore, the calculated vibrational wavenumbers are scaled with 0.955 and 0.977 for the vibrational wavenumbers above and below 1800  $\text{cm}^{-1}$  respectively [13]. Table 2 presents the calculated (un-scaled and scaled) vibrational wavenumbers, IR intensities and Raman activities along with the assignment of vibrational modes for the TPC. The Table also shows the observed infrared wavenumbers of TPC for comparison. The assignment of the fundamental vibrational modes is proposed on the basis of potential energy distribution using VEDA 4 program and the animation option of Gauss View graphical interface of Gaussian program. A detailed description of the normal modes based on PED is given in the last column of Table 2. TPC is composed of 16 atoms. Thus, the calculation gives forty two IR fundamental vibrations that belong to irreducible representations  $\Gamma_{\text{vib}} = 15A_1 + 7A_2 + 6B_1 + 14B_2$  of the  $C_{2v}$  point group of TPC. The absence of imaginary wavenumbers in the calculated vibrational spectrum confirms that the optimized structure corresponds to the minimum energy on the potential energy surface. The  $A_1$  and  $B_2$  irreducible representations correspond to stretching, ring deformation, and in-plane bending vibrations, while  $A_2$  and  $B_1$  correspond to ring, torsion and out of plane bending vibrations. The normal modes associated with  $A_1$ ,  $B_1$  and  $B_2$  symmetries are IR and Raman active, while the modes associated with  $A_2$  symmetry are Raman active but IR inactive.

The vibrational wavenumbers and the corresponding intensities obtained from B3LYP/6-311++G(d,p) calculations were used to simulate the IR and Raman spectra of the title molecule. For simulation, pure Lorentzian band shape with a bandwidth of full width and half maximum (FWHM) of 10  $\text{cm}^{-1}$  was used to plot the calculated IR and Raman spectra. The experimental and simulated IR spectra of TPC molecule are presented in Figs. 2, while the Raman spectra are shown in Fig. 3. These Figures clearly show the spectral characteristics of the title molecule. Calculated Raman activities ( $S_i$ ) were converted to relative Raman intensities ( $I_i$ ) using the following equation (1) derived from the intensity theory of Raman scattering [29, 30].

$$I_i = \frac{f(\nu_0 - \nu_i)^4 S_i}{\nu_i [1 - \exp(-\frac{h\nu_i}{kT})]} - 1$$

Where  $\nu_0$  is the laser exciting wavenumber in  $\text{cm}^{-1}$ ,  $\nu_i$  is the vibrational wavenumber of the  $i^{\text{th}}$  normal mode, and  $f$  is a suitable common normalization factor for all peak intensities,  $10^{-4}$ .  $h$ ,  $k$ ,  $c$  and  $T$  are Planck and Boltzman constants, speed of light and temperature in Kelvin, respectively.

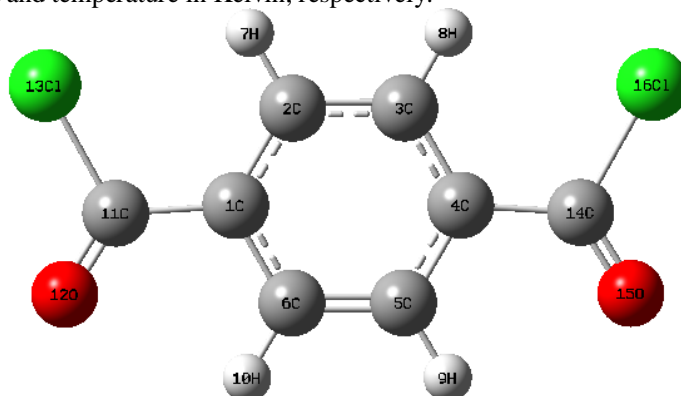


Figure 1. Optimized molecular structure of terephthaloyl chloride.

Table 1: The calculated optimized geometrical parameters<sup>a</sup> for terephthaloylchloride.

Bond lengths(Å)		Bond Angles(°)		Dihedral Angles(°)	
C <sub>1</sub> -C <sub>2</sub>	1.397	C <sub>2</sub> C <sub>1</sub> C <sub>6</sub>	119.8	C <sub>6</sub> C <sub>1</sub> C <sub>2</sub> C <sub>3</sub>	0.0
C <sub>1</sub> -C <sub>6</sub>	1.404	C <sub>2</sub> C <sub>1</sub> C <sub>11</sub>	123.7	C <sub>6</sub> C <sub>1</sub> C <sub>2</sub> C <sub>7</sub>	180.0
C <sub>1</sub> -C <sub>11</sub>	1.490	C <sub>6</sub> C <sub>1</sub> C <sub>11</sub>	116.5	C <sub>11</sub> C <sub>1</sub> C <sub>2</sub> C <sub>3</sub>	180.0
C <sub>2</sub> -C <sub>3</sub>	1.390	C <sub>1</sub> C <sub>2</sub> C <sub>3</sub>	120.1	C <sub>11</sub> C <sub>1</sub> C <sub>2</sub> C <sub>7</sub>	0.0
C <sub>2</sub> -H <sub>7</sub>	1.081	C <sub>1</sub> C <sub>2</sub> H <sub>7</sub>	120.1	C <sub>2</sub> C <sub>1</sub> C <sub>6</sub> C <sub>5</sub>	0.0
C <sub>3</sub> -C <sub>4</sub>	1.397	C <sub>3</sub> C <sub>2</sub> H <sub>7</sub>	119.8	C <sub>2</sub> C <sub>1</sub> C <sub>6</sub> H <sub>10</sub>	180.0
C <sub>3</sub> -H <sub>8</sub>	1.081	C <sub>2</sub> C <sub>3</sub> C <sub>4</sub>	120.1	C <sub>11</sub> C <sub>1</sub> C <sub>6</sub> C <sub>5</sub>	180.0
C <sub>4</sub> -C <sub>5</sub>	1.404	C <sub>2</sub> C <sub>3</sub> H <sub>8</sub>	119.8	C <sub>11</sub> C <sub>1</sub> C <sub>6</sub> H <sub>10</sub>	0.0
C <sub>4</sub> -C <sub>14</sub>	1.490	C <sub>4</sub> C <sub>3</sub> H <sub>8</sub>	120.1	C <sub>2</sub> C <sub>1</sub> C <sub>11</sub> O <sub>12</sub>	180.0
C <sub>5</sub> -C <sub>6</sub>	1.385	C <sub>3</sub> C <sub>4</sub> C <sub>5</sub>	119.8	C <sub>2</sub> C <sub>1</sub> C <sub>11</sub> Cl <sub>15</sub>	0.0
C <sub>5</sub> -H <sub>9</sub>	1.082	C <sub>3</sub> C <sub>4</sub> C <sub>14</sub>	123.7	C <sub>6</sub> C <sub>1</sub> C <sub>11</sub> O <sub>12</sub>	0.0
C <sub>6</sub> -H <sub>10</sub>	1.082	C <sub>5</sub> C <sub>4</sub> C <sub>14</sub>	116.5	C <sub>6</sub> C <sub>1</sub> C <sub>11</sub> Cl <sub>15</sub>	180.0
C <sub>11</sub> =O <sub>12</sub>	1.187	C <sub>4</sub> C <sub>5</sub> C <sub>6</sub>	120.1	C <sub>1</sub> C <sub>2</sub> C <sub>3</sub> C <sub>4</sub>	0.0
C <sub>11</sub> -Cl <sub>13</sub>	1.819	C <sub>4</sub> C <sub>5</sub> H <sub>9</sub>	119.2	C <sub>1</sub> C <sub>2</sub> C <sub>3</sub> H <sub>8</sub>	180.0
C <sub>14</sub> =O <sub>15</sub>	1.187	C <sub>6</sub> C <sub>5</sub> H <sub>9</sub>	120.7	C <sub>7</sub> C <sub>2</sub> C <sub>3</sub> C <sub>4</sub>	180.0
C <sub>14</sub> -Cl <sub>16</sub>	1.819	C <sub>1</sub> C <sub>6</sub> C <sub>5</sub>	120.1	C <sub>7</sub> C <sub>2</sub> C <sub>3</sub> H <sub>8</sub>	0.0
		C <sub>1</sub> C <sub>6</sub> H <sub>10</sub>	119.2	C <sub>2</sub> C <sub>3</sub> C <sub>4</sub> C <sub>5</sub>	0.0
		C <sub>5</sub> C <sub>6</sub> H <sub>10</sub>	120.7	C <sub>2</sub> C <sub>3</sub> C <sub>4</sub> C <sub>13</sub>	180.0
		C <sub>1</sub> C <sub>11</sub> O <sub>12</sub>	125.5	H <sub>8</sub> C <sub>3</sub> C <sub>4</sub> C <sub>5</sub>	180.0
		C <sub>1</sub> C <sub>11</sub> Cl <sub>13</sub>	115.5	H <sub>8</sub> C <sub>3</sub> C <sub>4</sub> C <sub>13</sub>	0.0
		O <sub>12</sub> C <sub>11</sub> Cl <sub>13</sub>	119.0	C <sub>3</sub> C <sub>4</sub> C <sub>5</sub> C <sub>6</sub>	0.0
		C <sub>4</sub> C <sub>14</sub> O <sub>15</sub>	125.5	C <sub>3</sub> C <sub>4</sub> C <sub>5</sub> H <sub>9</sub>	180.0
		C <sub>4</sub> C <sub>14</sub> Cl <sub>16</sub>	115.5	C <sub>13</sub> C <sub>4</sub> C <sub>5</sub> C <sub>6</sub>	180.0
		O <sub>15</sub> C <sub>14</sub> Cl <sub>16</sub>	119.0	C <sub>13</sub> C <sub>4</sub> C <sub>5</sub> H <sub>9</sub>	0.0
				C <sub>3</sub> C <sub>4</sub> C <sub>13</sub> O <sub>14</sub>	180.0
				C <sub>3</sub> C <sub>4</sub> C <sub>13</sub> Cl <sub>16</sub>	0.0
				C <sub>5</sub> C <sub>4</sub> C <sub>13</sub> O <sub>14</sub>	0.0
				C <sub>5</sub> C <sub>4</sub> C <sub>13</sub> Cl <sub>16</sub>	180.0
				C <sub>4</sub> C <sub>5</sub> C <sub>6</sub> C <sub>1</sub>	0.0
				C <sub>4</sub> C <sub>5</sub> C <sub>6</sub> H <sub>10</sub>	180.0
				H <sub>9</sub> C <sub>5</sub> C <sub>6</sub> C <sub>1</sub>	180.0
				H <sub>9</sub> C <sub>5</sub> C <sub>6</sub> H <sub>10</sub>	0.0

<sup>a</sup>The atom numbering is given in Fig.1.

**Table 2:** Experimental and corresponding scaled and unscaled theoretical vibrational wavenumbers ( $\text{cm}^{-1}$ ) of terephthaloylchloride.

No.	Sym.	Expt	$\nu^a$	$\nu^b$	$I_{\text{IR}}^c$	$I_{\text{R}}^d$	Assignment (PED $\geq$ 10%)
v <sub>1</sub>	A1	3101	3227	3082	0.37	83.85	$\nu_{\text{CH}}(99)$
v <sub>2</sub>	B2	3060	3216	3071	0.19	24.44	$\nu_{\text{CH}}(99)$
v <sub>3</sub>	A1	2987	3213	3069	0.00	105.49	$\nu_{\text{CH}}(99)$
v <sub>4</sub>	B2	2665	3201	3057	2.12	31.89	$\nu_{\text{CH}}(99)$
v <sub>5</sub>	A1	1763	1839	1756	514.60	297.53	$\nu_{\text{CO}}(92)$
v <sub>6</sub>	B2	1728	1836	1754	155.24	44.18	$\nu_{\text{CO}}(93)$
v <sub>7</sub>	A1	1690	1642	1605	1.54	421.58	$\nu_{\text{CC}}(67) + \delta_{\text{HCC}}(10)$
v <sub>8</sub>	B2	1570	1604	1567	16.13	0.98	$\nu_{\text{CC}}(55) + \delta_{\text{HCC}}(11)$
v <sub>9</sub>	B2	1505	1522	1487	11.20	0.18	$\delta_{\text{HCC}}(63) + \delta_{\text{CCC}}(13)$
v <sub>10</sub>	A1	1427	1431	1398	35.22	9.86	$\nu_{\text{CC}}(35) + \delta_{\text{HCC}}(30)$
v <sub>11</sub>	A1	1404	1346	1315	8.22	0.34	$\nu_{\text{CC}}(64)$
v <sub>12</sub>	B2	1290	1332	1301	0.39	0.62	$\delta_{\text{HCC}}(86)$
v <sub>13</sub>	A1	1198	1223	1195	20.64	37.26	$\nu_{\text{CC}}(59) + \delta_{\text{HCC}}(30)$
v <sub>14</sub>	B2	-	1202	1175	371.72	0.30	$\nu_{\text{C-C}}(35) + \delta_{\text{HCC}}(27)$
v <sub>15</sub>	A1	1134	1189	1162	44.82	157.85	$\nu_{\text{CC}}(43) + \delta_{\text{HCC}}(31)$
v <sub>16</sub>	A1	1115	1145	1118	2.02	4.03	$\nu_{\text{CC}}(17) + \delta_{\text{HCC}}(58)$
v <sub>17</sub>	B2	1019	1035	1011	0.49	0.00	$\nu_{\text{CCC}}(77)$
v <sub>18</sub>	A2	978	1015	992	In active	0.04	$\tau_{\text{HCCC}}(68) + \tau_{\text{CCCC}}(24)$
v <sub>19</sub>	A2	894	1003	980	In active	0.48	$\tau_{\text{HCCC}}(69) + \tau_{\text{CCCC}}(10)$
v <sub>20</sub>	A1	877	904	883	139.19	7.21	$\nu_{\text{CC}}(40) + \delta_{\text{CCC}}(22)$
v <sub>21</sub>	B1	853	885	865	33.06	0.00	$\tau_{\text{HCCC}}(71) + \tau_{\text{CCCC}}(16)$
v <sub>22</sub>	B2	798	861	841	520.45	2.77	$\nu_{\text{CC}}(12) + \nu_{\text{CCl}}(10) + \delta_{\text{OCCl}}(29) + \delta_{\text{CCC}}(20)$
v <sub>23</sub>	B1	780	859	839	0.67	0.01	$\tau_{\text{HCCC}}(93)$
v <sub>24</sub>	A2	732	774	756	In active	1.84	$\tau_{\text{CCCC}}(82)$
v <sub>25</sub>	A1	693	705	689	110.72	31.28	$\nu_{\text{CCl}}(13) + \delta_{\text{CCCl}}(58)$
v <sub>26</sub>	B1	656	669	654	44.17	0.01	$\delta_{\text{HCC}}(17) + \delta_{\text{CCC}}(76)$
v <sub>27</sub>	B2	639	647	632	1.60	6.68	$\nu_{\text{CC}}(11) + \delta_{\text{CCC}}(66)$
v <sub>28</sub>	A2	-	636	621	In active	0.77	$\delta_{\text{CCC}}(89)$
v <sub>29</sub>	B2	559	582	569	26.97	1.51	$\nu_{\text{CC}}(26) + \nu_{\text{CCl}}(14) + \delta_{\text{CCC}}(38)$
v <sub>30</sub>	A1	538	484	473	14.27	15.54	$\nu_{\text{CCl}}(41) + \delta_{\text{CCC}}(38)$
v <sub>31</sub>	B1	444	447	436	0.41	0.01	$\tau_{\text{CCCC}}(90)$
v <sub>32</sub>	B2	-	440	430	0.07	5.22	$\nu_{\text{CCl}}(32) + \delta_{\text{OCCl}}(56)$
v <sub>33</sub>	A2	-	414	405	In active	0.09	$\tau_{\text{HCCC}}(21) + \tau_{\text{CCCC}}(66)$
v <sub>34</sub>	A1	-	395	386	14.57	2.08	$\nu_{\text{CCl}}(32) + \delta_{\text{CCC}}(27)$
v <sub>35</sub>	B2	-	377	368	34.31	4.31	$\nu_{\text{CCl}}(41) + \delta_{\text{CCC}}(36)$
v <sub>36</sub>	A1	-	239	234	6.62	5.12	$\nu_{\text{CC}}(14) + \delta_{\text{CCC}}(56)$
v <sub>37</sub>	A2	-	232	227	In active	1.10	$\tau_{\text{CCCC}}(95)$
v <sub>38</sub>	B2	-	218	213	1.25	3.00	$\delta_{\text{CCC}}(10) + \delta_{\text{CCCl}}(85)$
v <sub>39</sub>	A1	-	118	115	3.31	0.72	$\delta_{\text{CCCl}}(87)$
v <sub>40</sub>	B1	-	75	73	5.00	0.02	$\tau_{\text{CCCC}}(87)$
v <sub>41</sub>	B1	-	44	43	0.13	0.75	$\tau_{\text{CCCl}}(90)$
v <sub>42</sub>	A2	-	28	28	In active	0.03	$\tau_{\text{CCCl}}(92)$

<sup>a</sup>Unscaled vibrational wavenumbers

<sup>b</sup>Scaled vibrational wavenumbers (scaled with 0.955 above 1800  $\text{cm}^{-1}$  and 0.977 under 1800  $\text{cm}^{-1}$ )

<sup>c</sup> $I_{\text{IR}}$ , calculated infrared intensities in  $\text{km mol}^{-1}$ .

<sup>d</sup> $I_{\text{R}}$ , calculated Raman intensities in  $\text{\AA}^4 \text{amu}^{-1}$ .

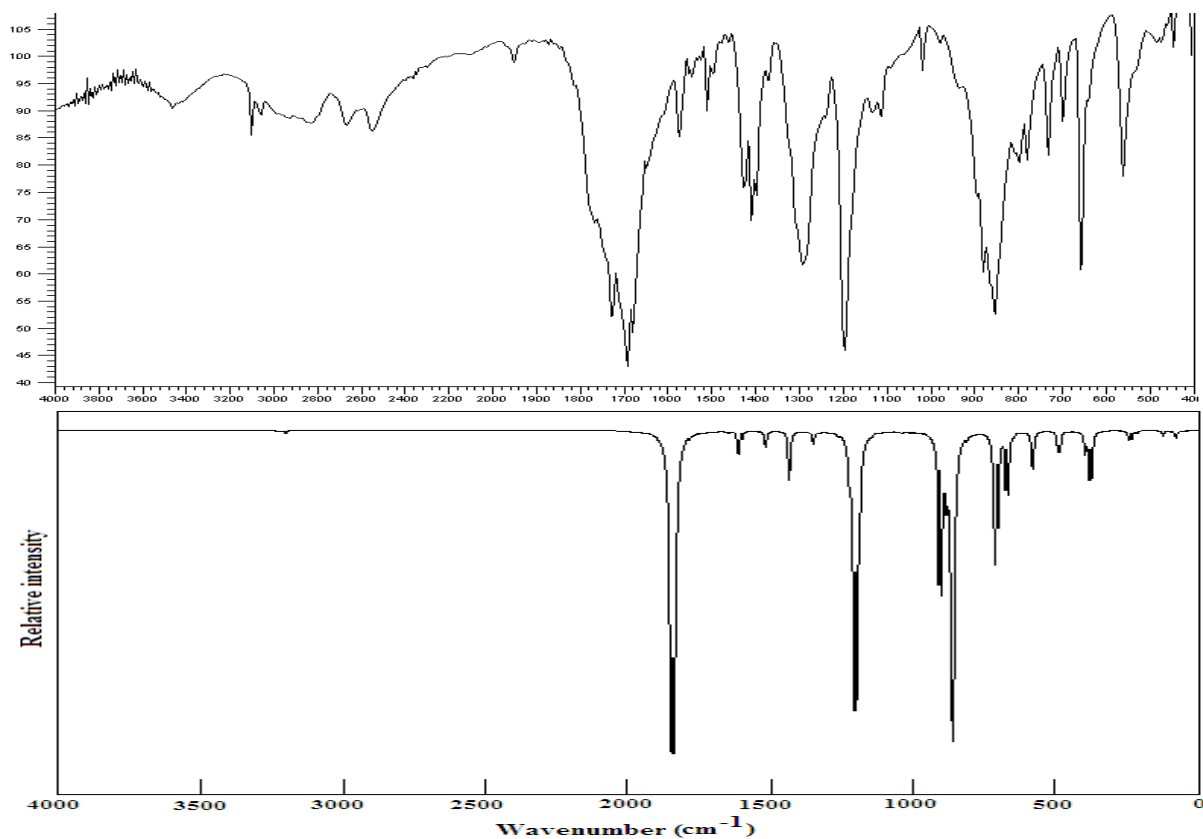


Figure 2: Experimental (top) and simulated (bottom) infrared spectra of terephthaloylchloride.

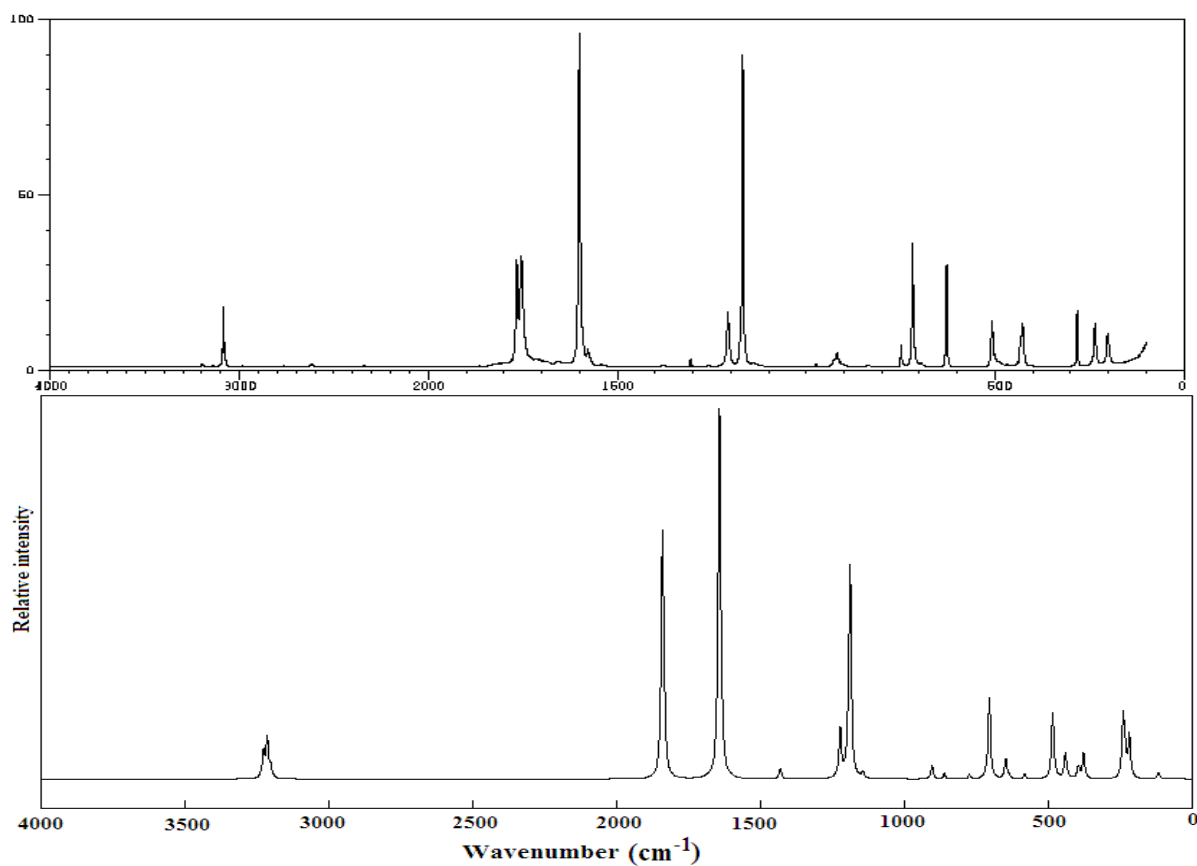


Figure 3: Experimental (top) and simulated (bottom) Raman spectra of terephthaloylchloride.

Generally, the aromatic C-H stretching modes appears in the region 3100 – 3000  $\text{cm}^{-1}$ [31]. In the present study, the bands at 3101, 3060, 2987 and 2665  $\text{cm}^{-1}$  in the FTIR spectrum of TLC (Fig. 2) are attributed to aromatic C-H stretching vibrations. These bands correspond to the calculated vibrational wavenumber at 3082, 3071, 3069, and 3057  $\text{cm}^{-1}$ , which show good correlation between experimental and theoretical vibrational wavenumbers. As evident from PED calculations presented in the last column of Table 2, these bands are pure stretching vibration having almost 99% contributions to the total PED. The IR vibrational and Raman spectra are dominated by high intensity bands at around 1700  $\text{cm}^{-1}$ . These bands are assigned to carbonyl (C=O) stretching frequency. The aromatic acid halides showed a strong C=O stretching absorption band in the region of 1800 – 1770  $\text{cm}^{-1}$ , and this band shows very small dependence on conjugation [31]. The calculated wavenumbers at 1756 and 1754  $\text{cm}^{-1}$  (with PED contributions of 92 and 93% respectively) corresponding to symmetric and asymmetric C=O stretching vibrations, appear at 1763 / 1728  $\text{cm}^{-1}$  in FTIR spectrum and at 1755  $\text{cm}^{-1}$  in the Raman spectrum of TPC.

### 4.3 Thermodynamic Parameters and Electronic Properties

In general, thermodynamic properties are useful for physicists and chemists and are important in the study of several molecular properties. Thus, on the basis of theoretical frequency calculation at B3LYP/6-311++G(d,p) level of theory, several standard statistical thermodynamic functions and rotational constants are obtained, and the data are presented in Table 3. The standard thermodynamic functions such as heat capacity and entropy increase with temperature because the intensity of molecular vibration increases with temperature. The variation of the heat capacity and entropy with temperature is presented in Fig. 4.

**Table 3:**Thecalculated thermodynamics parameters of terephthaloyl chloride.

SCF Energy (Hartree)	-1378.299288
Total Thermal Energy, $E_{\text{total}}$ (K cal mol <sup>-1</sup> )	69.870
Heat capacity at const. volume, $C_v$ (cal mol <sup>-1</sup> k <sup>-1</sup> )	37.678
Entropy, $S$ (cal mol <sup>-1</sup> k <sup>-1</sup> )	104.834
Vibrational energy, $E_{\text{vib}}$ (K cal mol <sup>-1</sup> )	68.092
Zero point vibrational energy, $E_0$ (K cal mol <sup>-1</sup> )	63.261
Rotational Constant (GHz)	
A	1.92734
B	0.30384
C	0.26246
Dipole moment (Debye)	
$\mu_x$	0.000
$\mu_y$	0.000
$\mu_z$	0.8983
$\mu_{\text{total}}$	0.8983

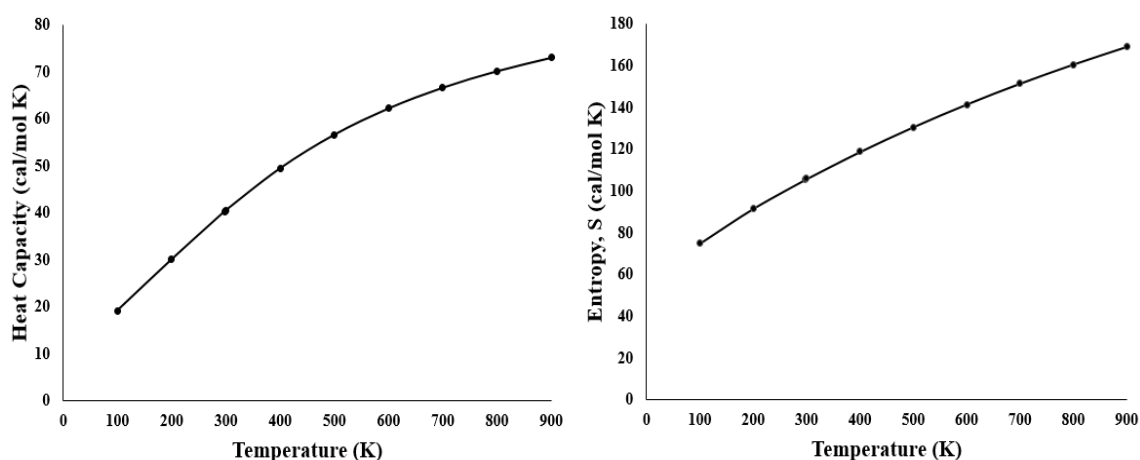


**Figure 4.** Variation of heat capacity and entropy with temperature.

The highest occupied molecular orbital (HOMO) and the lowest unoccupied molecular orbital (LUMO) and their properties are very useful for predicting the most reactive position in  $\pi$ -electron systems. They are also useful in explaining several types of reactions in a conjugated system [32]. The HOMO represents the ability to donate an electron, while the LUMO represents the ability to accept an electron. Thus, the energy of the HOMO is directly related to the ionization potential, while the LUMO energy is directly related to electron affinity, and the HOMO-LUMO energy gap is related to the molecular chemical stability. A molecule with a small HOMO-LUMO energy gap is more polarizable and is generally associated with high chemical reactivity [33, 34]. The HOMO and LUMO of TPC were calculated at B3LYP/6-311++G(d,p) level of theory. The 3D plots generated from the calculations are illustrated in Fig. 5, while the HOMO and LUMO energies and the HOMO-LUMO energy gaps are presented in Table 4. The HOMO and LUMO are delocalized over the entire molecules of TPC. In addition, the HOMO and LUMO energy values are used to calculate global chemical reactivity descriptors such as ionization potential (I), electron affinity (A), electronegativity ( $\chi$ ), chemical hardness ( $\eta$ ), chemical softness (S), chemical potential ( $\mu$ ), electrophilicity index ( $\omega$ ). The results are summarized in Table 4.

**Table 4:** Calculated HOMO and LUMO energies, HOMO-LUMO energy gap, ionization potential, electron affinity, electronegativity, chemical hardness, chemical potential, chemical softness and electrophilicity index of terephthaloyl chloride.

$E_{\text{HOMO}}$ (hartree)	-0.3086
$E_{\text{LUMO}}$ (hartree)	-0.1307
$E_{\text{HOMO}}$ (eV)	-8.3980
$E_{\text{LUMO}}$ (eV)	-3.5573
$ \Delta E  = E_{\text{HOMO}} - E_{\text{LUMO}}$ gap (eV)	4.8408
Ionization potentials, $I = -E_{\text{HOMO}}$ (eV)	8.3980
Electron affinity, $A = -E_{\text{LUMO}}$ (eV)	3.5573
Electronegativity, $\chi = (I + A)/2$ (eV)	5.9776
Chemical hardness, $\eta = (I - A)/2$ (eV)	2.4204
Chemical potential, $\mu = -(I + A)/2$ (eV)	-5.9776
Chemical softness, $S = 1/(2\eta)$ ( $\text{eV}^{-1}$ )	0.2066
Electrophilicity index, $\omega = \mu^2/2\eta$ (eV)	7.3815

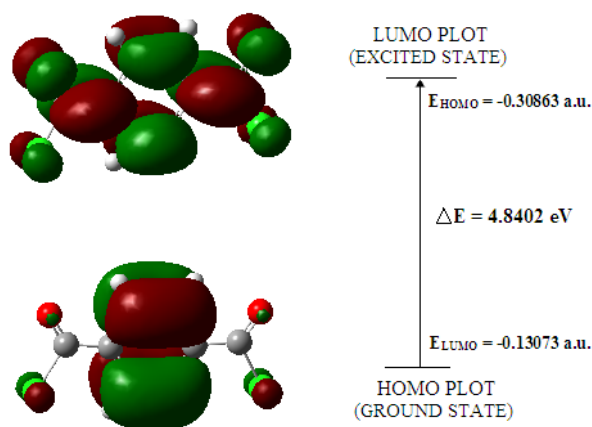


**Figure 5.** Frontier molecular orbitals (HOMO and LUMO) of terephthaloyl chloride.

#### 4.4 Molecular Electrostatic Potentials and Atomic Charges.

Atomic charges' calculation plays an important role in the applications of quantum chemical calculations to the molecular system because atomic charges affect molecular properties such as dipole moment, polarizability, and electronic structure. The charge distribution was calculated by Mulliken method for the equilibrium geometry of the TPC, and the results are illustrated in Fig. 6. The positive charges are mainly localized on hydrogen atoms, while the carbon atoms are found to be either positive or negative. The carbon atoms ( $C_1$  and  $C_4$ ) that are bonded to the carbonyl chloride groups are more positive than other carbons due to the partial polar nature of the carbonyl group ( $C=O$ ). The magnitude of oxygen atoms are  $-0.085e$ , while that of the two chlorine atoms are  $0.439e$ . In general, the result suggests that the oxygen atoms and the carbon atoms bonded to oxygen atoms are electron acceptor.

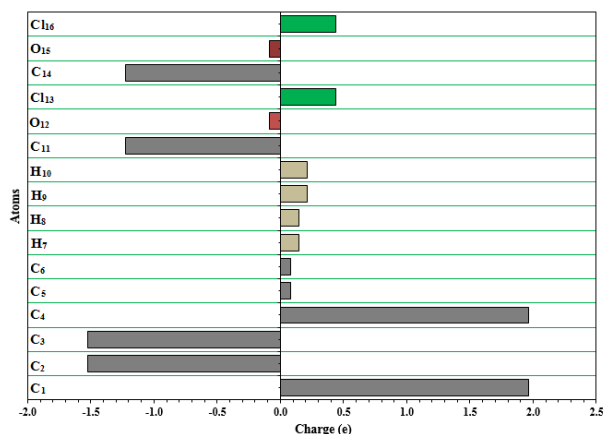


**Figure 6.** Mulliken atomic charge distribution of terephthaloyl chloride.

Molecular Electrostatic Potential (MEP) mapping is very important in the study of molecular interactions, prediction of relative sites for nucleophilic and electrophilic attack, molecular cluster and prediction wide range of macroscopic properties [35, 36]. To predict reactive sites for nucleophilic and electrophilic attack for TPC molecule, the MEP at the B3LYP/6-311++G(d,p) optimized geometry was calculated and the result is illustrated in Fig. 7. The electrostatic potentials at the surface are represented by different colors; red, blue and green represent the regions of negative, positive and zero electrostatic potentials respectively. In addition, the negative regions (red color) of MEP are related to electrophilic reactivity, and the positive regions (blue color) are related to the nucleophilic reactivity. As can be seen from Fig. 7, the negative electrostatic potentials are localized over the oxygen atoms, and are potential sites for electrophilic attack. The positive regions are localized around the hydrogen atoms. The green region corresponds to electrostatic potential halfway between the red and the blue and are potential sites for intermolecular interactions.

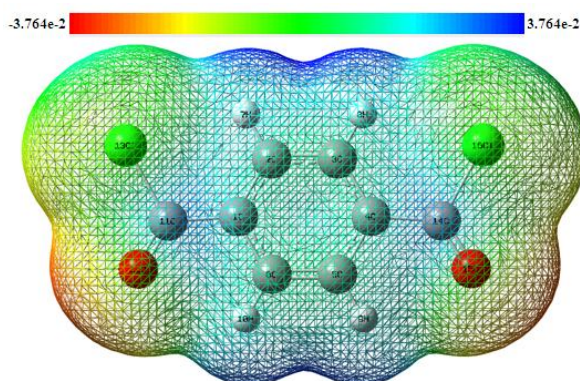


**Figure 7.** Molecular electrostatic potential energy surface (MEP) for terephthaloyl chloride.

## V. Conclusion

In this article, experimental FTIR has been recorded and detailed vibrational assignment based on potential energy distribution is presented for terephthaloyl chloride. The equilibrium geometry vibrational wavenumbers, thermodynamic and electronic properties of terephthaloyl chloride were theoretically examined. All the calculations were carried using the B3LYP density functional theory adopting 6-311++G(d,p) standard basis set. The scaled vibrational wavenumbers are in good agreement with the experimental FTIR wavenumbers. The simulated IR and Raman spectra exactly coincide with the experimental FTIR and FT-Raman spectra of the title molecule. The atomic charges, HOMO and LUMO energies, thermodynamic parameters and molecular electrostatic potentials of the TPC were determined and analyzed. The calculated thermodynamic data reveal that heat capacity and entropy increase with the temperature because the molecular vibration intensities increase with temperature. In general, we hope that the result of this present study will play an important in understanding of dynamics of this molecule.

## Acknowledgements

Facilities provided by Jubail Industrial College of Royal Commission for Jubail and Yanbu are gratefully acknowledged.

## References

- [1]. DuPont Specialty Chemical Intermediates. Terephthaloyl Chloride (<http://www.dupont.com/specintermediates/tcl.html> (accessed Aug 2006).
- [2]. J. M Garcia, F. C. Garcia, F. Serna, J. L. de la Pena, High performance aromatic polyamids, *Progress in Polymer Science*, 35 (5), 2010, 623–686.
- [3]. H. Ichiura, T. Seike, Y. Ohtani, Interfacial Polymerization of Functional Paper: Morphology of the Nylon Film Prepared on Paper Surfaces, *Ind. Eng. Chem. Res.*, 52, 2013, 9137–9144.
- [4]. C. H. Schmitz, M. Schmid, S. Gartner, H. Steinruck, J. M. Gottfried, M. Sokolowski Surface Polymerization of Poly(p-phenylene-terephthalamide) on Ag(111) Investigated by X-ray Photoelectron Spectroscopy and Scanning Tunneling Microscopy, *J. Phys. Chem. C*, 115, 2011, 18186–18194.
- [5]. S. R Long, M. L. Zhang, G. Zhang, X. J. Wang, J. Yang, Synthesis and characterization of poly(ethylene terephthalamide/hexamethyleneterephthalamide), *Journal of Macromolecular Science, Part A: Pure and Applied Chemistry*, 49(1), 2012, 67-72.
- [6]. S. J. Bae, M. K.Joo, Y. Jeong, S. W. Kim, W. Lee, Y. S. Sohn, B. Jeong, Gelation Behavior of Poly(ethylene glycol) and Polycaprolactone Triblock and Multiblock Copolymer Aqueous Solutions, *Macromolecules*, 39, 2006, 4873-4879.
- [7]. M. G. Zolotukhin, H. M. Colquhoun, L. G. Sestia, One-Pot Synthesis and Characterization of Soluble Poly(aryl ether-ketone) Having Pendant Carboxyl Groups, *Macromolecules* 36, 2003, 4766-4771.
- [8]. T. Fukumaru, Y. Saegusa, T. Fujigaya, N. Nakashima, Fabrication of Poly(p-phenylenebenzobisoxazole) Film Using a Soluble Poly(o-alkoxyphenylamide) as the Precursor Macromolecules, 47, 2014, 2088–2095.
- [9]. H. R. Kricheldorf, B. Fechner Polylactones. 59. Biodegradable Networks via Ring-Expansion Polymerization of Lactones and Lactides with a Spirocyclic Tin Initiator, *Biomacromolecules*, 3, 2002, 691-695.
- [10]. Z. Ekemen, H. Chang, Z. Ahmad, C. Bayram, Z. Rong, E. Baki Denkbaz, E. Stride, P. Vadgama, M. Edirisinghe Fabrication of Biomaterials via Controlled Protein Bubble Generation and Manipulation, *Biomacromolecules*, 12, 2011, 4291–4300.
- [11]. J. C. Williams, M. Ann B. Meador, L. McCorkle, C. Mueller, N. Wilmoth, Synthesis and Properties of Step-Growth Polyamide Aerogels Cross-linked with Triacid Chlorides, 26, 2014, 4163–4171.
- [12]. F. Zhang, Z. Jia, M. P. Srinivasan, Application of Direct Covalent Molecular Assembly in the Fabrication of Polyimide Ultrathin Films, *Langmuir* 2005, 21, 3389-3395.
- [13]. Y. Umar, A Comparative Study on the Molecular Structures and Vibrational Spectra of 2-, 3- and 4-Cyanopyridines by Density Functional Theory, *IOSR Journal of Applied Chemistry*, 8(7), 2015, 44-55.
- [14]. J. D. Magdaline, T. Chithambarathanu, Vibrational Spectra (FT-IR, FT-Raman), NBO and HOMO, LUMO Studies of 2-Thiophene Carboxylic Acid Based On Density Functional Method, *IOSR Journal of Applied Chemistry*, 8(5), 2015, 6-14.
- [15]. M.V.S. Prasad, N. U. Sri, V. Veeraiyah, A combined experimental and theoretical studies on FT-IR, FT-Raman and UV-Vis spectra of 2-chloro-3-quinolinecarboxaldehyde, *Spectrochimica Acta Part A: Molecular and Biomolecular Spectroscopy*, 118, 2015, 163-174.
- [16]. Y. Umar, Density functional theory calculations of the internal rotations and vibrational spectra of 2-, 3- and 4-formyl pyridine, *Spectrochimica Acta Part A: Molecular and Biomolecular Spectroscopy*, 71(5), 2009, 1907-1913.
- [17]. Y. Umar, Theoretical investigation of the structure and vibrational spectra of carbamoylazide, *Spectrochimica Acta Part A: Molecular and Biomolecular Spectroscopy*, 64(3), 2006, 568-573.
- [18]. Y. Umar, M.A. Morsy, Ab initio and DFT studies of the molecular structures and vibrational spectra of succinonitrile, *Spectrochimica Acta Part A: Molecular and Biomolecular Spectroscopy*, 66(4-5), 2007, 1133-1140.
- [19]. M. Bakiler, O. Bolukbasi, A. Yilmaz, An experimental and theoretical study of vibrational spectra of picolinamide, nicotinamide, and isonicotinamide, *Journal of Molecular Structure*, 826(1), 2007, 6-16.
- [20]. E. Güneş, C. Parlak, DFT, FT-Raman and FT-IR investigations of 5-methoxysalicylic acid, *Spectrochimica Acta Part A: Molecular and Biomolecular Spectroscopy*, 82(1), 2011, 504-514.
- [21]. SDBS Web: <http://sdb.sdb.aist.go.jp> (National Institute of Advanced Industrial Science and Technology, accessed on 14<sup>th</sup> July 2015).
- [22]. M. J. Frisch, et al, Gaussian, Inc., Wallingford CT, 2003.
- [23]. D. Becke, Density-functional thermochemistry. III. The role of exact exchange, *J. Chem. Phys.* 98, 1993, 5648-5653.
- [24]. Lee, W. Yang, R. G. Parr, Development of the Colle-Salvetti correlation-energy formula into a functional of the electron density, *Physical Review B*, 37, 1988, 785-789.
- [25]. R. Dennington II, T. Keith, J. Millam, et al. Gauss View, Version 3.09. (Semichem, Inc., Shawnee Mission, KS, 2003).
- [26]. M. H. Jamroz, Vibrational Energy Distribution Analysis: VEDA 4 Program Warsaw (2004).
- [27]. M. Kurt, P. Chinna Babu, N. Sundaraganesan, M. Cinar, M. Karabacak, Molecular structure, vibrational, UV and NBO analysis of 4-chloro-7-nitrobenzofurazan by DFT calculations, *Spectrochimica Acta Part A: Molecular and Biomolecular Spectroscopy*, 79(5), 2011, 1162-1170.
- [28]. J. Vipin Prasad, S.B. Rai, S.N. Thakur, Overtone spectroscopy of benzene derivatives using thermal lensing, *Chemical Physics Letters*, 164(6), 1989, 629-634.
- [29]. G. Keresztury, S. Holly, G. Besenyi, J. Varga, Aiying Wang, J.R. Durig, Vibrational spectra of monothiocarbamates-II. IR and Raman spectra, vibrational assignment, conformational analysis and ab initio calculations of S-methyl-N, N-dimethylthiocarbamate, *Spectrochimica Acta Part A: Molecular Spectroscopy*, 49(13-14), 1993, 2007-2017.
- [30]. G. Keresztury, J. M. Chalmers, Griffith P R (Eds), *Raman Spectroscopy: theory in Handbook of Vibrational Spectroscopy Vol 1*, John Wiley & sons Ltd New York, 2002.
- [31]. R. M. Silverstein, F. X. Webster, *Spectrometric identification of organic compounds* (Sixth edition, John Wiley and Sons, Inc. USA, 1998).
- [32]. M. Kurt, P. C. Babu, N. Sundaraganesan, M. Cinar, M. Karabacak, Molecular structure, vibrational, UV and NBO analysis of 4-chloro-7-nitrobenzofurazan by DFT calculations, *Spectrochimica Acta Part A* 79, 2011, 1162 – 1170.
- [33]. S. Gunasekaran, R.A. Balaji, S. Kumeresan, G. Anand, S. Srinivasan, Experimental and theoretical investigations of spectroscopic properties of N-acetyl-5-methoxytryptamine, *Can. J. Anal. Sci. Spectrosc.* 53, 2008, 149-160.
- [34]. D. F. V. Lewis, C. Ioannides, D. V. Parke, Interaction of a series of nitriles with the alcohol-inducible isoform of P450: Computer analysis of structure—activity relationships, *Xenobiotica*, 24(5), 1994, 401-408.
- [35]. J.S. Murray, K. Sen, *Molecular Electrostatic Potentials Concepts and Applications* Elsevier Science B.V, Amsterdam, 1996.
- [36]. L.G. Wade Jr., *Organic Chemistry*, sixth ed., Pearson Prentice Hall, New Jersey, 2006.